Title

Biolayer Interferometry Assay for Cyclin-Dependent Kinase-Cyclin Association Reveals Diverse Effects of Cdk2 Inhibitors on Cyclin Binding Kinetics

Journal

ACS Chemical Biology, 18(2)

ISSN

1554-8929

Authors

Tambo, Carrie S
Tripathi, Sarvind
Perera, B Gayani K
et al.

Publication Date

2023-02-17

DOI

10.1021/acschembio.3c00015

Peer reviewed

HHS Public Access

Author manuscript

ACS Chem Biol. Author manuscript; available in PMC 2023 March 21.

Published in final edited form as:

ACS Chem Biol. 2023 February 17; 18(2): 431–440. doi:10.1021/acschembio.3c00015.

Biolayer Interferometry Assay for Cyclin-Dependent Kinase-Cyclin Association Reveals Diverse Effects of Cdk2 Inhibitors on Cyclin Binding Kinetics

Carrie S. Tambo,
Department of Chemistry and Biochemistry, University of California, Santa Cruz, California 95064, United States

Sarvind Tripathi,
Department of Chemistry and Biochemistry, University of California, Santa Cruz, California 95064, United States

B. Gayani K. Perera,
Department of Chemistry, University of Washington, Seattle, Washington 98195, United States

Dustin J. Maly,
Department of Chemistry, University of Washington, Seattle, Washington 98195, United States; Department of Biochemistry, University of Washington, Seattle, Washington 98195, United States

Alexander J. Bridges,
Type6 Therapeutics Inc., Santa Clara, California 95051, United States

Gert Kiss,
Type6 Therapeutics Inc., Santa Clara, California 95051, United States

Seth M. Rubin
Department of Chemistry and Biochemistry, University of California, Santa Cruz, California 95064, United States

Abstract

Cyclin-dependent kinases (CDKs) are key mediators of cell proliferation and have been a subject of oncology drug discovery efforts for over two decades. Several CDK and activator cyclin family members have been implicated in regulating the cell division cycle. While it is thought that there are canonical CDK-cyclin pairing preferences, the extent of selectivity is unclear, and increasing evidence suggests that the cell-cycle CDKs can be activated by a pool of available

Corresponding Author: Seth M. Rubin – srubin@ucsc.edu.

ASSOCIATED CONTENT

Supporting Information

The Supporting Information is available free of charge at https://pubs.acs.org/doi/10.1021/acschembio.3c00015.

X-ray diffraction data and model refinement statistics (Table S1), additional data supporting BLI experiments, data analysis, and interpretation of results (Figures S1–S4), isothermal titration calorimetry data (Figure S5), and additional figure describing structure of the MC14-Cdk2 complex (Figure S6) (PDF)

The authors declare the following competing financial interest(s): S. Rubin and D. Maly disclose grants from Type6 Therapeutics related to CDK research. S. Rubin also discloses consulting fees from Type6 Therapeutics.

Complete contact information is available at: https://pubs.acs.org/10.1021/acschembio.3c00015

cyclins. The molecular details of CDK-cyclin specificity are not completely understood despite their importance for understanding cancer cell cycles and for pharmacological inhibition of cancer proliferation. We report here a biolayer interferometry assay that allows for facile quantification of CDK binding interactions with their cyclin activators. We applied this assay to measure the impact of Cdk2 inhibitors on Cyclin A (CycA) association and dissociation kinetics. We found that Type I inhibitors increase the affinity between Cdk2 and CycA by virtue of a slowed cyclin dissociation rate. In contrast, Type II inhibitors and other small-molecule Cdk2 binders have distinct effects on the CycA association and dissociation processes to decrease affinity. We propose that the differential impact of small molecules on the cyclin binding kinetics arises from the plasticity of the Cdk2 active site as the kinase transitions between active, intermediate, and inactive states.

Graphical Abstract

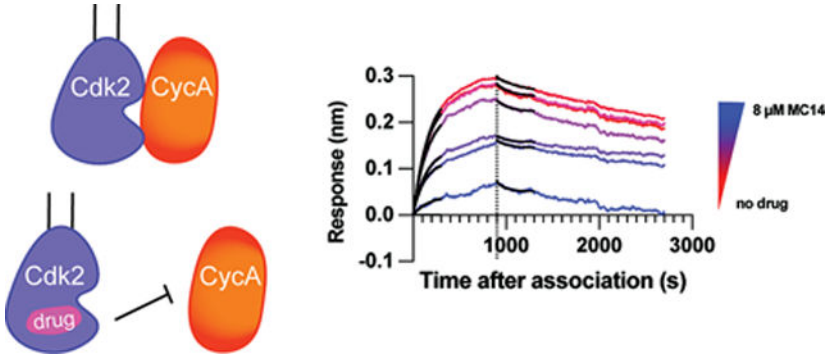

INTRODUCTION

Cyclin-dependent kinases (CDKs) control progression through the cell cycle and are prominent targets for cancer therapeutics due to their impact on proliferation. CDKs coordinate processes throughout the cell cycle by phosphorylating protein substrates to change their localization, stability, and binding interactions.[1–3] The cell-cycle CDKs are activated by binding of the cyclin subunit and by phosphorylation of a specific threonine in the kinase activation loop (A-loop), which shift the kinase from an inactive to an active state. The structural changes that occur upon cyclin binding and A-loop phosphorylation reposition the C-helix and A-loop to generate a conformation optimized for ATP binding, substrate binding, and catalysis.[3–6] The CDKs that control the cell cycle are often found in cells with specific cognate cyclin partners; for example, CycD pairs with Cdk4 and Cdk6, while CycA and CycE pair with Cdk2. Although these CDKs and cyclins have been extensively studied along with additional protein inhibitors and activators in the complex, the molecular determinants of these preferential enzymatic pairings and differences in intrinsic activities remain unclear. Recent studies have also brought attention to the significance of noncanonical pairings and activators. These noncanonical pairings occur in the context of proliferating cancer cells, which may have imbalanced levels of CDKs, cyclins, or their regulators,[7] in situations in which a CDK is genetically inactivated,[8] and in the context of CDK inhibitor treatment, which may alter the distribution of subunits in CDK complexes.[9–12] Despite the impact of CDK-cyclin association on the cell cycle and

proliferation, there have been few studies that quantify CDK-cyclin affinity to understand the factors that drive and modulate binding and their binding preferences.[13–16]

Inactivation of the retinoblastoma tumor suppressor protein by CDK phosphorylation is required for S phase entry and is commonly deregulated in proliferating cancer cells.[17] The deregulation of CDK pathways in cancer has motivated significant research into the development of CDK inhibitors as therapeutics.[18,19] The success of palbociclib and related Cdk4/6 inhibitors in the clinic is motivating evidence that intervention in cell-cycle control pathways is a viable strategy for reducing cancer progression.[20,21] On the other hand, the intrinsic and acquired resistance of cancers to Cdk4/6 inhibitors points to the need for development of molecules toward other targets, especially Cdk2, which can compensate for Cdk4/6 and can also be a primary driver of cancer cell proliferation.[22] Creating specific Cdk2 inhibitors that target the ATP binding site in the active kinase conformation (Type I inhibitors) has been challenging due to structural homology with Cdk1.[23,24] Cdk1 inhibition in most contexts results in toxicity, which is consistent with past observations that knockout of Cdk1 does not generate viable mice.[25,26] Interestingly, several Type I inhibitors discriminate in their binding between monomeric Cdk2 and Cdk1, while most of that selectivity is lost when targeting the active CDK-cyclin heterodimers.[24] There have also been reports of a Type II inhibitor, AUZ 454 (or K03861), which binds monomer Cdk2 and stabilizes an inactive conformation of the A-loop DFG motif,[27] and of a class of compounds developed specifically to inhibit Cdk2-cyclin association.[28] Another recent study found that the plant alkaloid and approved drug for leukemia known as homoharringtonine (HHT) inhibits Cdk2-CycA association and promotes autophagic degradation of Cdk2.[29] A deepened understanding of how inhibitor-kinase association impacts cyclin association and vice versa will be critical for assessing the pharmacological relevance of any given agent. Interestingly, it has been demonstrated that inhibitor and cyclin binding are thermodynamically coupled due to the impact of both on the Cdk2 conformation.[5]

Here, we describe a biolayer interferometry (BLI) assay for measuring CDK-cyclin binding, and we directly quantify the affinity and kinetics of Cdk2-CycA association. We report the effects of different classes of Cdk2 inhibitors and identify differential impacts on association and dissociation kinetics. Remarkably, we found that molecules can inhibit CycA binding through distinct kinetic mechanisms, and we use structural insights to explain how compound perturbations to the conformation of Cdk2 impact the CycA binding interactions.

RESULTS

BLI Assay for Measuring Cdk2-CycA Binding Kinetics.

We developed a BLI assay to measure Cdk2-CycA interactions. BLI enables observation of association and dissociation kinetics, is high throughput, and requires minimal quantities of purified reagents (~100 ng per assay).[30,31] In the BLI format, the smaller protein (here Cdk2) is immobilized onto the biosensor through an affinity tag. Upon dipping the loaded biosensor into an analyte (CycA) solution, analyte binding is detected as a real-time interferogram throughout the duration of the experiment. We attempted Cdk2

immobilization using either a GST fusion protein tag or a biotinylated preparation of the enzyme at various concentrations and found that 750 ng/mL is optimal to detect changes in response while preventing saturation of the sensor (Figure 1a,b). For GST fusion, Cdk2 was cloned and expressed in *E. coli* with a GST affinity tag, which was used both for protein purification and for immobilization through the use of an anti-GST biosensor. For biotinylation, the GST fusion tag was cleaved during purification, and the Cdk2 was covalently modified with an N-terminal biotinylated peptide using the sortase enzyme.[32] Biotinylated Cdk2 was immobilized in our assays with streptavidin biosensors. When using either immobilization strategy, we found that nonspecific binding (NSB) was a reoccurring issue. The NSB was observable as a BLI response that occurred upon dipping an empty biosensor, i.e., not loaded with Cdk2, into CycA solution. The NSB was remedied by the addition of 2 mg/mL BSA and 0.2% Tween to the assay running buffer, and in the case of using the anti-GST biosensors, by the insertion of a blocking step using 1 μM GST to block any accessible sites on the biosensor. We found that further increasing the Tween concentration, use of other nonionic or ionic detergents, or addition of Mg^{2+} to the buffer did not improve the assay.

For both the GST-Cdk2 and biotin-Cdk2 experiments measuring CycA binding kinetics, the immobilized ligand on the biosensor was dipped into the analyte at different concentrations. A range of CycA concentrations from 500 to 8 nM, in 2-fold step dilutions, yielded data with an optimal response signal and variation in k_{obs}, which is the observed rate constant during the association step (Figure 1c,d). We monitored association of CycA by the increase in the BLI response for 900 s, but we found that the data, particularly at higher CycA and Cdk2 concentrations, do not fit well to a single kinetic step (Figures S1 and S2). We suspect that there is a second slower process that is either nonspecific binding between the proteins or a slower specific binding event that is coupled to a structural transition in either Cdk2 or CycA. We focused our analysis on the fast association step that had a greater, concentration-dependent response. For simplicity, we determined k_{obs} and the maximum response by fitting the first 300 s of data to a single k_{obs} using the Octet BLI system software (Figure S1). To measure dissociation rate constants (k_d), the immobilized Cdk2 was dipped in buffer, and dissociation of CycA was detected through the decrease in the BLI response. For the dissociation step, we fit the first 400 s of data and determined the k_d by assuming that the response returns to zero (Figure S1). Fitting the data in this manner, we determined similar values of k_d, the association rate constant (k_a, determined from k_{obs} and k_d), and binding constant (K_d) for the two different immobilized Cdk2 constructs (Figure 1c,d). The maximum response for immobilized biotin-Cdk2 biosensor was consistently greater than that for the immobilized GST-Cdk2 biosensor when compared at similar protein concentrations, and we also observed less variation in the fit parameters across the different concentrations and replicates for the biotin-Cdk2 experiments. We found that the K_d determined from the kinetic rate constants was similar to the K_d determined from the CycA concentration dependence of the BLI response signal at equilibrium (Figure S2). We obtained similar binding parameters when biotin-Cdk2 was loaded at either a 3-fold lower or higher concentration (Figure S2), and when Cdk2 was phosphorylated on its activation loop by CDK-activating kinase prior to final purification (Figure S3). Therefore,

for all subsequent studies, we used the unphosphorylated biotin-Cdk2 immobilized on the biosensor and used a loading concentration of 750 ng/mL.

Cdk2 Inhibitors Change CycA Association and Dissociation Rates.

We applied the optimized BLI assay to study the influence of Cdk2 small-molecule inhibitors on the kinetics of CycA association and dissociation. Considering the allosteric coupling that has been observed between structural features of the Cdk2 kinase,[5] we hypothesized that distinct Cdk2 inhibitors could influence the kinetics of cyclin assembly by stabilizing different Cdk2 structural conformations. A panel of Cdk2 inhibitors that vary in their pharmacophore and their mode of action was used along with palbociclib, a Cdk4/6 specific inhibitor, as a negative control (Figure 2). In one approach, we introduced a high concentration of each compound (2 μM) at the baseline step in the BLI assay that occurs after loading Cdk2 but before addition of CycA (i.e., at ~500 s in Figure 1b), and 2 μM of each compound was present during subsequent steps. 2 μM was chosen based on reported kinase activity inhibition constants, and the intention was to keep a saturating concentration of the compound during the association and dissociation steps such that the experiments reflected only the kinetics of CycA binding to compound-bound Cdk2 complexes. We did not detect a BLI response when the Cdk2 biosensor is introduced to the compound alone during the preincubation step, suggesting that under our assay conditions, the signal is not sensitive to the subtle changes in the molecular weight or conformation induced by the small-molecule binding to kinase alone.

We observed changes in the affinity and kinetics of CycA binding for all of the tested compounds, apart from the negative control palbociclib, which does not bind Cdk2 at the tested concentration (Figure 2).[20] We tested two Type I Cdk2 inhibitors that bind the active conformation of the kinase at the ATP site. Dinaciclib is a pan-CDK inhibitor that targets Cdk1/2/5/9,[33] while BMS265246 targets Cdk1/2/4.[34] We found that the Type I inhibitors significantly increased the affinity (smaller K_d) of CycA binding to Cdk2, around 3-fold for dinaciclib and 6-fold for BMS265246 (Figure 2a,b,f). For both compounds, the increase in affinity occurred through a decrease in the dissociation rate constant k_d, while the k_a was not significantly changed. The observation of cooperativity between Type I ATP-site inhibitors and CycA binding was previously observed through comparison of inhibitor affinities for Cdk2 alone vs Cdk2-CycA complexes.[5] Here, we demonstrate the same cooperativity through direct measurement of CycA affinity and show that it manifests through a slowed dissociation.

We tested two compounds in the assay that are known to compete with binding of activating cyclins. We found using the BLI assay that AUZ 454, which binds preferentially to monomeric Cdk2 over Cdk2-CycA,[27] significantly decreased CycA affinity by ~10-fold (Figure 2d,f). Interestingly, AUZ 454 influences both the association and dissociation steps. AUZ 454 increased both k_a and k_d, but the relatively greater increase in k_d results in a weaker K_d. The nearly ~30-fold faster dissociation is particularly striking, and in the presence of AUZ 454, the dissociation curves could be fit without assuming return to zero signal. We suspect that the residual signal is from nonspecific interactions with the Cdk2-loaded sensor, some of which may be protein aggregation. Other cyclin binding

competitive compounds have been reported which are not canonical Type II inhibitors in that they do not induce an inactive conformation of the DFG motif.[28,29] We tested Merck compound 14 (MC14), which is a quinoline-based compound developed from a screen of CycA binding inhibitors.[28] It was previously reported that MC14 binds Cdk2 with 5 nM affinity, as determined from temperature-dependent circular dichroism, and destabilizes purified Cdk2-CycA complexes as determined by thermostability experiments.[28] In the presence of 2 μM MC14, we found a decreased response for CycA association across the CycA concentration range (Figure 2e). Although we typically found some variation in response across all our BLI experiments, the decreased response with 2 μM MC14 was reproducible and further supported by titrating MC14 (Figure 3). The decreased response is consistent with less CycA binding to the sensor. Although fitting the smaller signal yields less precise measurements (Figure 2f), the residual signal displays similar kinetics. We conclude that MC14 occludes CycA association and that the residual signal is generated from the population of compound-free kinase on the biosensor.

Measuring the Compound Dose Response on CycA Association.

We next adapted the BLI assay to measure dose responses of the compounds by maintaining the CycA concentration at 125 nM and varying compound concentration across the eight biosensors in an experiment (Figure 3). As in the CycA titration experiments, the compound was introduced to immobilize Cdk2 for 180 s after Cdk2 loading on the biosensor and prior to exposure to CycA, and the compound was maintained in solution during CycA association and dissociation. Using this approach, we assume that a compound-concentration-dependent equilibrium with Cdk2 is present for the duration of the experiment such that the observed rates only depend on the specific kinetics of CycA binding. In support of this assumption, experiments using longer 30 min preincubation times showed similar results (not shown). As we titrated the Type I inhibitor BMS265246, the slope of the dissociation curve noticeably flattens and the k_d decreases (Figure 3a). Although the dynamic range of the k_d change was rather limited, we found an EC_{50} ~ 10 nM. We tested AUZ 454 in the dose response format and also found that we could measure the compound-dependent changes in k_d (Figure 3b). We fit the dose response curves to determine IC_{50} for CycA inhibition and used our measured K_d for Cdk2-CycA association to calculate corresponding K_i values. We emphasize that these K_i values quantify the potency of the compound at inhibiting CycA binding to Cdk2 (rather than catalytic activity). We found a similar but slightly tighter K_i value for AUZ 454 (K_i = 10 ± 7 nM) compared to the reported K_d value for Cdk2 (K_d = 50 ± 4 nM).[27] In the dose response experiment with MC14, increasing compound concentration correlated with a lower BLI response in a dose-dependent manner (Figure 3c). Our interpretation is that CycA cannot associate with the fraction of Cdk2 on the biosensor that is bound by the compound, and the remaining compound-free Cdk2 associates with CycA with the same binding kinetics as observed in the absence of compound. We found a slightly weaker MC14 K_i for CycA inhibition (K_i = 20 ± 10 nM) compared to the previously reported affinity of MC14 for Cdk2 (K_d = 5 nM).[28] Unlike the compounds, titration of ATP or the mimetic ATP-gamma-S did not generate any changes to the kinetics of CycA binding (Figure S4). We also tested the reported Cdk2-CycA inhibitor HHT in the dose response assay format, but we found no strong effects at concentrations as high as 32 μM HHT (Figure 3d). We also could not observe

any heat signal above background when titrating HHT with Cdk2 in an isothermal titration calorimetry experiment (Figure S5), so we found no evidence of HHT-Cdk2 interaction.

We tested in the dose response format the impact of exposing compounds to a preformed Cdk2-CycA complex, rather than incubating compounds with Cdk2 prior to CycA association (Figure 4). In these experiments, Cdk2-loaded biosensors were dipped into wells of CycA only (Figure 4, left step) and then into CycA with the compound to allow for compound incubation in the presence of CycA (middle step), and then into the compound only to allow CycA to dissociate (right step). In the titration with AUZ 454, we observed little change in response during the coincubation period (Figure 4a, middle step) and an increase in the CycA dissociation rate when CycA was removed (Figure 4a, right step). This result is consistent with our interpretation that AUZ 454 forms a ternary complex with Cdk2-CycA but stimulates CycA dissociation. We suggest that in the presence of CycA in the middle step, CycA dissociates and re-associates with the Cdk2 biosensor, as the overall equilibrium favors the ternary complex in the presence of high CycA concentrations in solution relative to the K_d. However, once CycA is removed from solution, the Cdk2-CycA-AUZ 454 ternary complex is both kinetically and thermodynamically labile, and the remaining CycA on the biosensor dissociates. When CycA was introduced prior to MC14 (Figure 4b), we observed no change during the coincubation period and CycA dissociation kinetics resembled CycA dissociation in the absence of compound. This observation supports the conclusions that CycA and MC14 binding are mutually exclusive and that CycA dissociation is sufficiently slow such that MC14 cannot bind Cdk2 during the coincubation period. A possible alternative conclusion is that MC14 binds the preformed dimer but does not impact the CycA dissociation rate. However, we disfavor this interpretation in light of the exclusion of CycA by MC14 (Figure 3c) and the structural data presented below. Finally, we found that addition of BMS265246 following CycA still resulted in a slower CycA dissociation rate (Figure 4c), which is consistent with the type I inhibitor binding and stabilizing the preformed kinase dimer.

Structural Changes Explain the Differences in Cyclin Binding Kinetics in the Presence of CDK Inhibitors.

We used available and new structural data to understand the basis for the different effects of AUZ 454 and MC14 on CycA binding kinetics. In particular, we were interested in identifying any structural perturbations, induced by the compounds binding to monomer Cdk2, that may explain why AUZ 454 increases both k_a and k_d and why MC14 decreases k_a such that we could not detect the association signal. Comparison of the AUZ 454-Cdk2 structure (PDB ID: 5A14) with the apoCdk2 structure (PDB ID: 1HCK) reveals a significant rotation and shift of the C-helix that is induced through specific interactions with the compound (Figure 5a).[27,35] Specifically, Leu55 in Cdk2 makes van der Waals contacts with the terminal trifluoromethylphenyl ring, and the sidechain of Glu51 in the C-helix makes two hydrogen bonds with the NHs on the urea linker that connects the terminal trifluoromethylphenyl ring with the 4-amino-phenyl ether scaffold. These interactions move the C-helix more than 6 angstroms toward the “in” conformation relative to apoCdk2, which places Leu55 and Glu51 in nearly the same positions as in the active Cdk2-CycA structure (PDB: 1FIN) (Figure 5b).[4] We propose that the increase in k_a results from the priming effect

of AUZ 454 on the C-helix in that it properly positions the C-helix for CycA association. Notably, the interactions made by AUZ 454 and Cdk2 are for the most part compatible with the CycA-bound structure (Figure 5b), explaining why we still observe significant affinity of CycA in the presence of the compound. The main exception is that the position of the sidechain of F148 in the DFG motif in the active Cdk2-CycA structure clashes with the terminal trifluoromethylphenyl ring of AUZ 454 in the AUZ 454-Cdk2 structure. There is no available structure of AUZ 454 bound to a Cdk2-CycA complex, and beyond a few residues that follow the DFG motif, the activation loop is not ordered in the AUZ 454-Cdk2 structure. We propose that the perturbation to the activation loop conformation, which in the active structure makes a number of stabilizing contacts with CycA, is the likely source of the increase in the k_d. We also note that the β-sheet in the N-terminal lobe of the kinase domain is rotated slightly away from CycA in the AUZ 454-Cdk2 structure compared to the apoCdk2 structure (Figure 5a). While the source of this rotation is not obvious, it may be another reason why the cyclin dissociation is more rapid.

We determined the structure of MC14 bound to Cdk2 by soaking crystals of apoCdk2 with compound (Table S1, Figure 5c,d). As previously observed for the similar compound MC2,[28] MC14 binds the hinge at the ATP site through its hydroxyl group on the 4-OH-phenyl, and the chloro group on the 4-Cl-styryl extends toward the C-helix and contacts residues in the C-helix and A-loop (Figure S6). The C-helix position in the compound-bound structure is slightly tilted further “out” relative to apoCdk2 (Figure 5c). More importantly, the position of the chloro group on the 4-Cl-styryl in MC14 would clearly clash with the “in” conformation of the C-helix in the active Cdk2-CycA dimer (Figure 5d), and the small hydrophobic pocket occupied by the 4-Cl-styryl is to a large extent occluded in the heterodimer structure (Figure S6). These clashes explain the incompatibility of MC14 and CycA binding and why we observe no CycA association when Cdk2 is preincubated with the compound and vice-versa.

DISCUSSION

We describe here a method for direct measurement of CDK-cyclin binding kinetics and affinity using BLI. Benefits of this approach include the high throughput, the low protein reagent requirements, and the ability to directly observe the association and dissociation processes. Our studies demonstrate that Cdk2 inhibitors can affect CycA assembly through different mechanisms that impact both the association and dissociation rates. The Type I inhibitors tested, dinaciclib and BMS265246, increased affinity by decreasing k_d. Our observation is consistent with the previous discovery of an allosteric network that couples binding of Cdk2 ATP-site inhibitors and CycA.[5] Interestingly, we do not observe any influence of ATP or ATP-γ-S on CycA binding. This result suggests that contacts made by Type I inhibitors other than those that mimic ATP drive the coupling to the CycA binding site. In contrast to Type I inhibitors, we found that cyclin competitors overall reduce affinity of CycA to Cdk2 but vary in their modes of how they affect the rate constants k_a and k_d. When Cdk2 is bound by the Type II inhibitor AUZ 454, we observed an increase in both k_a and k_d of CycA, while another compound MC14 inhibited CycA association when the drug is bound. These effects arise through the effect of the compounds on the conformations of

the C-helix and A-loop, the two primary structural elements that couple CycA binding to increased catalytic activity.

Previous approaches have exploited a cyclin-mediated change in fluorescence of Cdk2-bound MANT(*N*-methylanthraniloyl)-ATP to measure k_{obs} for the cyclin association step.[14,16] By analyzing the dependence of k_{obs} on cyclin concentration, the dissociation rate constant k_d and binding constant K_d could be indirectly determined. The affinity we measure here for CycA (K_d = 1.9 ± 0.8 nM) is 25-fold tighter than that reported in two MANT-ATP studies (~50 nM).[14,16] We have considered three possible reasons for this discrepancy, which relate to advantages and disadvantages of the BLI assay. First, to achieve sufficient signals, MANT-ATP measurements were necessarily carried out at CycA concentrations in the range of 100–1000 nM, and therefore determining k_d from the ligand concentration dependence of k_{obs} (i.e., $k_{obs} = k_a[\text{CycA}] + k_d$) required linear regression analysis under conditions in which k_a[CycA] is ~100–1000× greater than k_d. The more direct measurement of k_d in the BLI experiment circumvents this large extrapolation to the *y*-intercept that is required in the MANT-ATP data analysis and is potentially error prone.

In comparison to the previous MANT-ATP experiments, a weakness of the BLI approach in our experiments is that the slow cyclin dissociation introduces challenges to directly measuring k_d. As noted, apart from the experiments using AUZ 454, we could only reliably fit the data assuming that the response signal returns to zero; however, as seen in those AUZ 454 experiments, it is more likely that the signal returns to a nonzero baseline from an effect such as nonspecific protein aggregation on the biosensor. As a result, we believe that our k_d values may be underestimated as smaller than the true values, which is consistent with us measuring a tighter K_d. Finally, considering BLI detects interactions with Cdk2 tethered to the surface, we may have measured slower dissociation and greater affinity because of CycA rapidly re-binding to a high local concentration of Cdk2. To try to detect this avidity effect, we varied the Cdk2 concentration up to 10-fold during loading, but we observed only a 2-fold increase in k_d between the lowest and highest loading concentrations (Figure S2b). It may be that there is an avidity effect that could be reduced even further at lower Cdk2 concentration, but the lowest Cdk2 concentration that can be loaded in the assay is limited by the weakened BLI signal. We did find that at a lower ligand loading concentration, data fitting to a single exponential kinetic model was improved, suggesting that the observed nonspecific signal at higher Cdk2 and CycA concentrations may result from surface tethering (Figure S2c). It should also be noted that one MANT-ATP study showed a rapid initial increase in fluorescence, which was attributed to cyclin association with k_a 100-fold greater than our measurement.[14,16] We did not observe such an initial rapid association event using BLI.

Increasing evidence points to potential advantages of Cdk2 inhibitors that target inactive monomer Cdk2 rather than the active Cdk2-CycA dimer. First, it has been found that several ATP-site orthosteric inhibitors achieve greater selectivity for Cdk2 over Cdk1 upon binding the inactive conformation.[24] Second, if targeting the inactive Cdk2 monomer inhibits cyclin association, the resulting redistribution of CDK-cyclin complexes in the cell may generate additional outputs beyond Cdk2 inhibition. For example, we and others have found that the Cdk4/6 inhibitor palbociclib can indirectly inhibit Cdk2 by inducing the formation of

Cdk2 complexes including CIP/KIP protein inhibitors.[10,12] Our data suggest that cyclin competitive compounds achieve CycA inhibition through different kinetic mechanisms. For example, the Type II inhibitor AUZ 454 increases the CycA dissociation rate, and we propose this destabilization results from the small molecule occluding the most stable conformation of the CycA-bound activation loop (Figure 5b). The fact that AUZ 454 also increases the CycA association rate suggests the compatibility of AUZ 454 and CycA in a ternary complex with Cdk2. However, this enhancement of association results in only a maximum ~10-fold decrease in affinity under saturating conditions of compound. In contrast, MC14 completely blocks CycA association under saturating conditions and appears mutually exclusive with CycA when in complex with Cdk2 (Figures 3c and 4b). We anticipate that the BLI assay described here will facilitate deeper exploration of CDK-cyclin signaling through providing a better understanding of how small molecules interact with and perturb CDK-cyclin binding.

METHODS

Protein Expression and Purification.

Full-length human Cdk2 was expressed as a GST fusion protein from a PGEX vector in BL21-DE3 *E. coli* for 16 h at 20 °C using 1 mM IPTG for induction. Cells were pelleted by centrifugation and lysed using an Emulsiflex C3 cell disruptor (Avestin) in a buffer containing 25 mM Tris pH 8.0, 200 mM NaCl, 1 mM DTT, and 1 mM PMSF. The protein was then purified using Glutathione Sepharose 4B (Cytvia) affinity and anion exchange (Source Q, Cytvia) chromatography. Following elution from the anion exchange column, protein was cleaved overnight with 1% GST-TEV by mass and passed back over the glutathione Sepharose column to remove free GST and GST-TEV enzyme. Cdk2 was then concentrated for final purification using a Superdex 75 (Cytvia) size-exclusion chromatography column equilibrated in 25 mM Tris pH 8.0, 200 mM NaCl, and 1 mM DTT. Protein eluted as a single peak and was aliquoted and stored in 10% glycerol. GST-CycA (human CycA1, residues 173–465) was purified similarly to Cdk2. To generate Cdk2 phosphorylated on its activation loop, GST-Cdk2 was co-expressed with an untagged yeast CDK activating kinase and purified similar to as described for unphosphorylated Cdk2.[5]

To generate biotinylated Cdk2, we used sortase labeling as described,[32] utilizing the N-terminal glycine that is left following TEV cleavage. 500 μg of Cdk2 was reacted with 7 μg of a synthetic biotin-LPETGG peptide and a final concentration of 5 μM purified His-tagged sortase in a final reaction volume of 500 μL. The reaction was incubated for 18 h at 4 °C. Following the reaction, the Cdk2 was purified again by passing over Ni^{2+}-NTA and Superdex 75 columns and was stored as above.

Inhibitor Compounds.

AUZ 454, AZD5438, BMS265246, dinaciclib, HHT, and palbociclib were purchased from Selleckchem.com. MC14 was synthesized using methods previously described.[28]

Biolayer Interferometry.

BLI experiments were performed using an eight-channel Octet-RED96e (Santorius). Experiments were performed in an assay buffer containing 25 mM Tris pH 8.0, 150 mM NaCl, 1 mM DTT, 2 mg/mL BSA, and 0.2% (v/v) Tween. Samples were formatted in a 96-well plate with each well containing 200 μL. For each experiment, we used eight streptavidin biosensor tips (Santorius) that were loaded with the biotinylated Cdk2 ligand and then dipped into CycA analyte at varying CycA concentration and compound concentration. The ligand concentration at loading was 750 ng/mL for unphosphorylated Cdk2 (both GST and biotin labeled) and 1000 ng/mL for phosphorylated Cdk2. All experiments were accompanied by reference measurements using unloaded streptavidin tips dipped into the same analyte-containing wells. Experiments in which analyte concentration was varied also contained a zero-analyte reference. Data were processed and fit using Octet software version 7 (Santorius), except the data in Figure S1 were fit as described in the caption using Kaleidagraph v5 (Synergy Software). Before fitting, all datasets were reference-subtracted, aligned on the y axis through their respective baselines, aligned for interstep correction through their respective dissociation steps, and finally smoothened using Savitzy–Golay filtering. In a particular experiment, each of the sensorgrams corresponding to a different concentration of analyte or compound was fit locally using a 1:1 binding model. The first 300 s of association and 400 s of dissociation were used in the fit (Figure S1). In experiments in which the CycA concentration was varied, the rate and dissociation constants were averaged across the set of sensorgrams and the replicate experiment sensorgrams (14 sensorgrams in total). In the dose response experiments, averages were taken across three replicates at each compound concentration, and the reported K_i values are averages of the K_i values determined by fitting each of three replicates. K_i was calculated using the equation $K_i = IC_{50}/([CycA]/K_D + 1)$, where IC_{50} is the fit value for the dose response curve determined using GraphPad Prism, [CycA] is the CycA concentration used in the experiment (125 nM), and K_d was 2 nM as determined in Figure 2.

Isothermal Titration Calorimetry (ITC).

ITC was performed with a MicroCal VP-ITC system at 25 °C. Purified Cdk2 was concentrated and dialyzed into a buffer containing 25 mM Tris (pH 8.0), 150 mM NaCl, and 1 mM DTT. The compounds were diluted from a 10 mM DMSO stock into the dialysis buffer and loaded into the cell. A background control experiment was performed titrating Cdk2 into buffer containing the same amount of DMSO as present in the compound experiments. The concentrations of Cdk2 (300–400 μM) and compounds (15–30 μM) are indicated in Figure S5. Data were fit using the MicroCal Origin software package.

X-ray Crystallography.

Cdk2 was crystallized following size-exclusion chromatography by the sitting drop method at 22 °C. Unliganded Cdk2 crystals were grown by mixing 1 μL of protein (10 mg/mL) with an equal volume of reservoir solution (0.2 M NaCl, 100 mM MES pH 6.0, and 20% PEG 6000). Following growth, crystals were incubated overnight with 1 mM MC14 dissolved in mother liquor supplemented with 15% glycerol before flash freezing them in liquid nitrogen. Data were collected at 100 K from a single crystal at the Advanced light

source (ALS) Beamline 5.0.1, which is managed by the Berkeley Center for Structural Biology. Diffraction data from the Cdk2-MC14 soaked crystals were indexed using XDS[36] and integrated and scaled using AIMLESS[37] in the CCP4 program suite.[38] The protein crystallized in the $P2_12_12_1$ space group, and the final structure contains one molecule of Cdk2 bound to MC14 in the asymmetric unit. Unliganded Cdk2 (PDB: 4EK3) was used as a search model in molecular replacement calculations using Phaser.[39] The Phenix suite was used for structure refinement.[40] All reflections were used for refinement except for 5% excluded for R_{free} calculations. The structural model was revised in real space with the program COOT[41] based on sigma-A weighted $2F_o$-F_c and F_o-F_c electron density maps. The final refinement statistics are given in Table S1. The structure factors and coordinates of the Cdk2-MC14 complex crystal structure were deposited in the Protein Data Bank under accession number 8CUR.

Supplementary Material

Refer to Web version on PubMed Central for supplementary material.

ACKNOWLEDGMENTS

This work was supported by grants from the National Institutes of Health to S. Rubin (R01 CA228413 and S10OD027012) and D. Maly (R01 GM086858). Work was also supported by sponsored research agreements between Type6 Therapeutics and University of California, Santa Cruz (S. Rubin PI) and University of Washington (D. Maly PI). The Berkeley Center for Structural Biology is supported in part by the Howard Hughes Medical Institute. The Advanced Light Source is a Department of Energy Office of Science User Facility under Contract No. DE-AC02-05CH11231. The Pilatus detector on 5.0.1 was funded under NIH grant S10OD021832. The ALS-ENABLE beamlines are supported in part by the National Institutes of Health, National Institute of General Medical Sciences, grant P30 GM124169. We thank N. Levinson (UMN Medical School) for the CDK-activating kinase expression plasmid.

REFERENCES

(1). Malumbres M Cyclin-dependent kinases. Genome Biol. 2014, 15, 122. [PubMed: 25180339]

(2). Morgan DO Cyclin-dependent kinases: engines, clocks, and microprocessors. Annu. Rev. Cell Dev. Biol. 1997, 13, 261–291. [PubMed: 9442875]

(3). Wood DJ; Endicott JA Structural insights into the functional diversity of the CDK-cyclin family. Open Biol. 2018, 8, No. 180112. [PubMed: 30185601]

(4). Jeffrey PD; Russo AA; Polyak K; Gibbs E; Hurwitz J; Massague J; Pavletich NP Mechanism of CDK activation revealed by the structure of a cyclinA-CDK2 complex. Nature 1995, 376, 313–320. [PubMed: 7630397]

(5). Majumdar A; Burban DJ; Muretta JM; Thompson AR; Engel TA; Rasmussen DM; Subrahmanian MV; Veglia G; Thomas DD; Levinson NM Allostery governs Cdk2 activation and differential recognition of CDK inhibitors. Nat. Chem. Biol. 2021, 17, 456–464. [PubMed: 33526892]

(6). Russo AA; Jeffrey PD; Pavletich NP Structural basis of cyclin-dependent kinase activation by phosphorylation. Nat. Struct. Biol. 1996, 3, 696–700. [PubMed: 8756328]

(7). Chaikovsky AC; Li C; Jeng EE; Loebell S; Lee MC; Murray CW; Cheng R; Demeter J; Swaney DL; Chen SH; et al. The AMBRA1 E3 ligase adaptor regulates the stability of cyclin D. Nature 2021, 592, 794–798. [PubMed: 33854239]

(8). Aleem E; Kiyokawa H; Kaldis P Cdc2-cyclin E complexes regulate the G1/S phase transition. Nat. Cell Biol. 2005, 7, 831–836. [PubMed: 16007079]

(9). Herrera-Abreu MT; Palafox M; Asghar U; Rivas MA; Cutts RJ; Garcia-Murillas I; Pearson A; Guzman M; Rodriguez O; Grueso J; et al. Early Adaptation and Acquired Resistance to CDK4/6 Inhibition in Estrogen Receptor-Positive Breast Cancer. Cancer Res. 2016, 76, 2301–2313. [PubMed: 27020857]

(10). Guiley KZ; Stevenson JW; Lou K; Barkovich KJ; Kumarasamy V; Wijeratne TU; Bunch KL; Tripathi S; Knudsen ES; Witkiewicz AK; et al. p27 allosterically activates cyclin-dependent kinase 4 and antagonizes palbociclib inhibition. Science 2019, 366, No. eaaw2106. [PubMed: 31831640]

(11). Li Q; Jiang B; Guo J; Shao H; Del Priore IS; Chang Q; Kudo R; Li Z; Razavi P; Liu B; et al. INK4 tumor suppressor proteins mediate resistance to CDK4/6 kinase inhibitors. Cancer Discovery 2022, 12, 356. [PubMed: 34544752]

(12). Pack LR; Daigh LH; Chung M; Meyer T Clinical CDK4/6 inhibitors induce selective and immediate dissociation of p21 from cyclin D-CDK4 to inhibit CDK2. Nat. Commun. 2021, 12, 3356. [PubMed: 34099663]

(13). Bloom J; Cross FR Multiple levels of cyclin specificity in cell-cycle control. Nat. Rev. Mol. Cell Biol. 2007, 8, 149–160. [PubMed: 17245415]

(14). Brown NR; Noble ME; Lawrie AM; Morris MC; Tunnah P; Divita G; Johnson LN; Endicott JA Effects of phosphorylation of threonine 160 on cyclin-dependent kinase 2 structure and activity. J. Biol. Chem. 1999, 274, 8746–8756. [PubMed: 10085115]

(15). Heitz F; Morris MC; Fesquet D; Cavadore JC; Doree M; Divita G Interactions of cyclins with cyclin-dependent kinases: a common interactive mechanism. Biochemistry 1997, 36, 4995–5003. [PubMed: 9125522]

(16). Morris MC; Gondeau C; Tainer JA; Divita G Kinetic mechanism of activation of the Cdk2/cyclin A complex. Key role of the C-lobe of the Cdk. J. Biol. Chem. 2002, 277, 23847–23853. [PubMed: 11959850]

(17). Rubin SM; Sage J; Skotheim JM Integrating Old and New Paradigms of G1/S Control. Mol. Cell 2020, 80, 183–192. [PubMed: 32946743]

(18). Otto T; Sicinski P Cell cycle proteins as promising targets in cancer therapy. Nat. Rev. Cancer 2017, 17, 93–115. [PubMed: 28127048]

(19). Sherr CJ; Beach D; Shapiro GI Targeting CDK4 and CDK6: From Discovery to Therapy. Cancer Discovery 2016, 6, 353–367. [PubMed: 26658964]

(20). Toogood PL; Harvey PJ; Repine JT; Sheehan DJ; VanderWel SN; Zhou H; Keller PR; McNamara DJ; Sherry D; Zhu T; et al. Discovery of a potent and selective inhibitor of cyclin-dependent kinase 4/6. J. Med. Chem. 2005, 48, 2388–2406. [PubMed: 15801831]

(21). Finn RS; Martin M; Rugo HS; Jones S; Im SA; Gelmon K; Harbeck N; Lipatov ON; Walshe JM; Moulder S; et al. Palbociclib and Letrozole in Advanced Breast Cancer. N. Engl. J. Med. 2016, 375, 1925–1936. [PubMed: 27959613]

(22). Alvarez-Fernandez M; Malumbres M Mechanisms of Sensitivity and Resistance to CDK4/6 Inhibition. Cancer Cell 2020, 37, 514–529. [PubMed: 32289274]

(23). Brown NR; Korolchuk S; Martin MP; Stanley WA; Moukhametzianov R; Noble MEM; Endicott JA CDK1 structures reveal conserved and unique features of the essential cell cycle CDK. Nat. Commun. 2015, 6, 6769. [PubMed: 25864384]

(24). Wood DJ; Korolchuk S; Tatum NJ; Wang LZ; Endicott JA; Noble MEM; Martin MP Differences in the Conformational Energy Landscape of CDK1 and CDK2 Suggest a Mechanism for Achieving Selective CDK Inhibition. Cell Chem. Biol. 2019, 26, 121–130.e5. [PubMed: 30472117]

(25). Diril MK; Ratnacaram CK; Padmakumar VC; Du T; Wasser M; Coppola V; Tessarollo L; Kaldis P Cyclin-dependent kinase 1 (Cdk1) is essential for cell division and suppression of DNA re-replication but not for liver regeneration. Proc. Natl. Acad. Sci. U. S. A. 2012, 109, 3826–3831. [PubMed: 22355113]

(26). Santamaria D; Barriere C; Cerqueira A; Hunt S; Tardy C; Newton K; Caceres JF; Dubus P; Malumbres M; Barbacid M Cdk1 is sufficient to drive the mammalian cell cycle. Nature 2007, 448, 811–815. [PubMed: 17700700]

(27). Alexander LT; Mobitz H; Drueckes P; Savitsky P; Fedorov O; Elkins JM; Deane CM; Cowan-Jacob SW; Knapp S Type II Inhibitors Targeting CDK2. ACS Chem. Biol. 2015, 10, 2116–2125. [PubMed: 26158339]

(28). Deng Y; Shipps GW Jr.; Zhao L; Siddiqui MA; Popovici-Muller J; Curran PJ; Duca JS; Hruza AW; Fischmann TO; Madison VS; et al. Modulating the interaction between CDK2 and cyclin

A with a quinoline-based inhibitor. Bioorg. Med. Chem. Lett. 2014, 24, 199–203. [PubMed: 24332088]

(29). Zhang J; Gan Y; Li H; Yin J; He X; Lin L; Xu S; Fang Z; Kim BW; Gao L; et al. Inhibition of the CDK2 and Cyclin A complex leads to autophagic degradation of CDK2 in cancer cells. Nat. Commun. 2022, 13, 2835. [PubMed: 35595767]

(30). Abdiche Y; Malashock D; Pinkerton A; Pons J Determining kinetics and affinities of protein interactions using a parallel real-time label-free biosensor, the Octet. Anal. Biochem. 2008, 377, 209–217. [PubMed: 18405656]

(31). Wilson JL; Scott IM; McMurry JL Optical biosensing: Kinetics of protein A-IGG binding using biolayer interferometry. Biochem. Mol. Biol. Educ. 2010, 38, 400–407. [PubMed: 21567869]

(32). Theile CS; Witte MD; Blom AE; Kundrat L; Ploegh HL; Guimaraes CP Site-specific N-terminal labeling of proteins using sortase-mediated reactions. Nat. Protoc. 2013, 8, 1800–1807. [PubMed: 23989674]

(33). Parry D; Guzi T; Shanahan F; Davis N; Prabhavalkar D; Wiswell D; Seghezzi W; Paruch K; Dwyer MP; Doll R; et al. Dinaciclib (SCH 727965), a novel and potent cyclin-dependent kinase inhibitor. Mol. Cancer Ther. 2010, 9, 2344–2353. [PubMed: 20663931]

(34). Misra RN; Xiao H; Rawlins DB; Shan W; Kellar KA; Mulheron JG; Sack JS; Tokarski JS; Kimball SD; Webster KR 1H-Pyrazolo[3,4-b]pyridine inhibitors of cyclin-dependent kinases: highly potent 2,6-Difluorophenacyl analogues. Bioorg. Med. Chem. Lett. 2003, 13, 2405–2408. [PubMed: 12824044]

(35). Schulze-Gahmen U; De Bondt HL; Kim SH High-resolution crystal structures of human cyclin-dependent kinase 2 with and without ATP: bound waters and natural ligand as guides for inhibitor design. J. Med. Chem. 1996, 39, 4540–4546. [PubMed: 8917641]

(36). Kabsch W Integration, scaling, space-group assignment and post-refinement. Acta Crystallogr., Sect. D: Biol. Crystallogr. 2010, 66, 133–144. [PubMed: 20124693]

(37). Evans P Scaling and assessment of data quality. Acta Crystallogr., Sect. D: Biol. Crystallogr. 2006, 62, 72–82. [PubMed: 16369096]

(38). Winn MD; Ballard CC; Cowtan KD; Dodson EJ; Emsley P; Evans PR; Keegan RM; Krissinel EB; Leslie AG; McCoy A; et al. Overview of the CCP4 suite and current developments. Acta Crystallogr., Sect. D: Biol. Crystallogr. 2011, 67, 235–242. [PubMed: 21460441]

(39). McCoy AJ; Grosse-Kunstleve RW; Adams PD; Winn MD; Storoni LC; Read RJ Phaser crystallographic software. J. Appl. Crystallogr. 2007, 40, 658–674. [PubMed: 19461840]

(40). Adams PD; Afonine PV; Bunkoczi G; Chen VB; Davis IW; Echols N; Headd JJ; Hung LW; Kapral GJ; Grosse-Kunstleve RW; et al. PHENIX: a comprehensive Python-based system for macromolecular structure solution. Acta Crystallogr., Sect. D: Biol. Crystallogr. 2010, 66, 213–221. [PubMed: 20124702]

(41). Emsley P; Cowtan K Coot: model-building tools for molecular graphics. Acta Crystallogr., Sect. D: Biol. Crystallogr. 2004, 60, 2126–2132. [PubMed: 15572765]

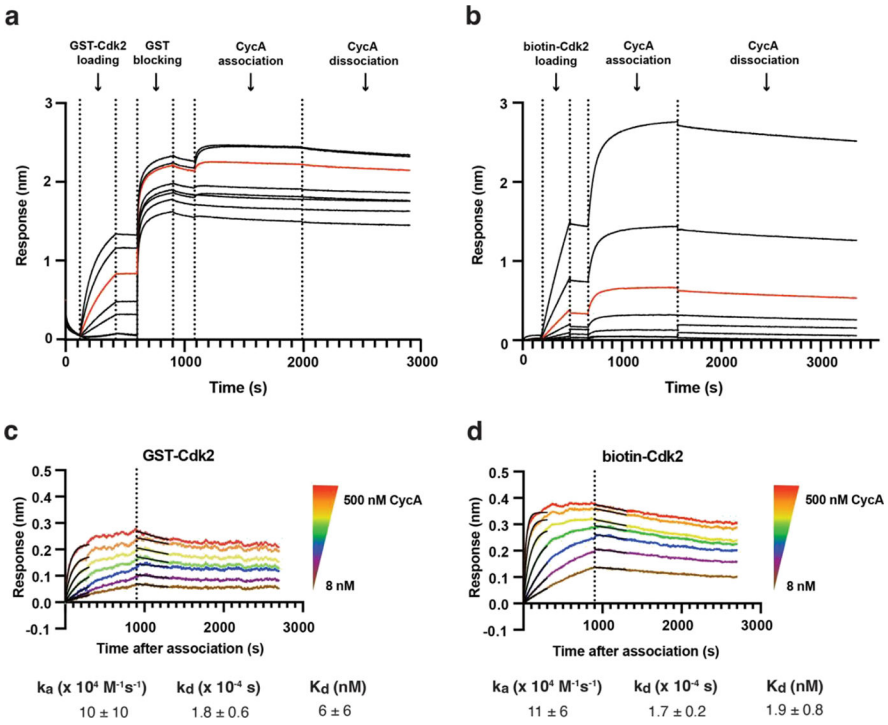

Figure 1.

BLI assay measures kinetics of Cdk2-CycA binding. (a,b) Full BLI sensorgrams that show response as a function of experiment time. The different curves represent different Cdk2 loading concentrations. The experiments with the concentration used in subsequent experiments (750 ng/mL GST-Cdk2 and 750 ng/mL biotin-Cdk2) are shown in red. (c,d) Association and dissociation steps of BLI assays using GST-Cdk2 (c) and biotin-Cdk2 (d). The concentration of CycA is varied in these experiments in 2-fold dilutions, and each sensorgram is double-referenced by subtracting both a zero ligand (Cdk2) and zero analyte (CycA) sensorgram. Each set of sensorgrams corresponds to one of two replicate experiments performed under each condition. The rate constants (k_a and k_d) and dissociation constant ($K_d = k_d/k_a$) were calculated for each sensorgram, and then, the fit parameters were averaged across all the sensorgrams corresponding to different CycA concentrations in both the performed replicates (14 sensorgrams total). The standard deviation is reported as error.

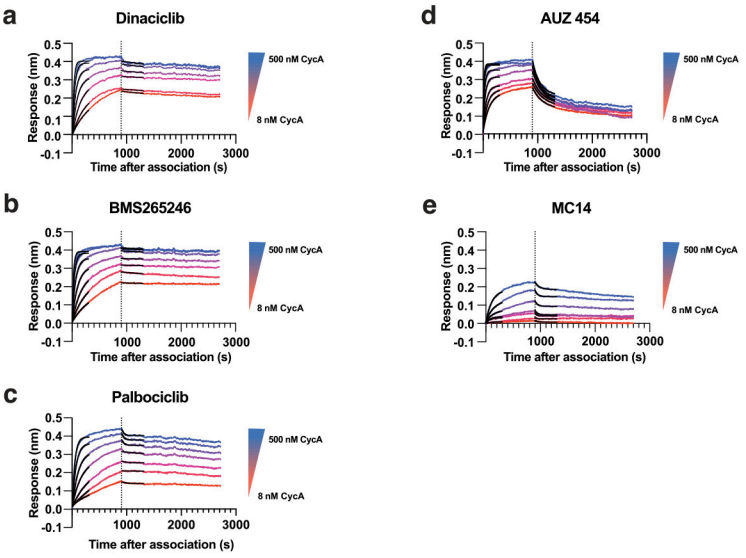

f

	k_a (x 10^4 $M^{-1}s^{-1}$)	k_d (x 10^{-4} s)	K_d (nM)
No drug	11 ± 6	1.7 ± 0.2	1.9 ± 0.8
Dinaciclib	14 ± 7	0.7 ± 0.2*	0.6 ± 0.3*
BMS265246	14 ± 8	0.4 ± 0.2*	0.3 ± 0.1*
AUZ 454	30 ± 10*	50 ± 10*	20 ± 10*
MC14	20 ± 20†	7 ± 4†	8 ± 7†
Palbociclib	11 ± 2	1.3 ± 0.5	2.2 ± 1.5

* $p < 0.0001$, comparison to no drug
† calculated from residual signal

Figure 2.

BLI assays measuring the effects of compounds on CycA binding kinetics. (a–e) In each experiment, biotin-Cdk2 was immobilized at a concentration of 750 ng/mL, and CycA concentration is varied as in Figure 1c,d. 2 μM compound was added to the buffer during the equilibration step preceding CycA addition and maintained throughout the association and dissociation steps. The set of sensorgrams in each panel shows the CycA association and dissociation steps of each BLI experiment. Each set of sensorgrams corresponds to one of two replicate experiments performed under each condition. The rate constants (k_a and k_d) and dissociation constant ($K_d = k_d/k_a$) were calculated for each sensorgram, and then, the fit parameters were averaged across all the sensorgrams corresponding to different CycA concentrations in both the performed replicates (14 sensorgrams total). The standard deviation is reported as error. (f) Table summarizing fitting of kinetic data.

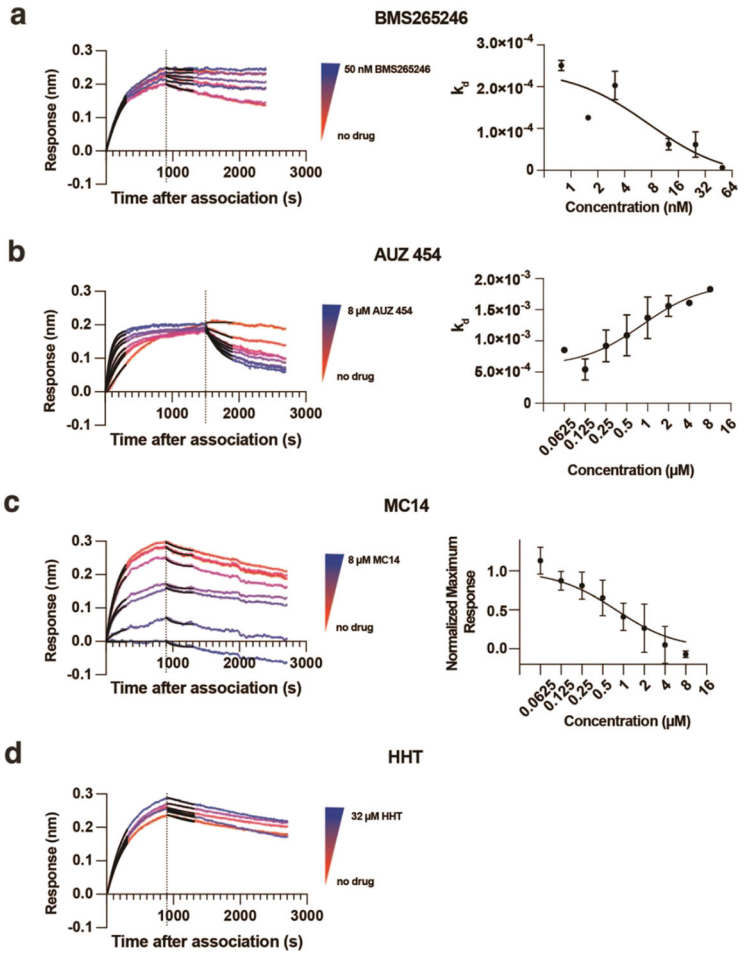

Figure 3.

(a–d) Dose response BLI measurements of Cdk2 inhibitors. The concentration of the indicated compound was varied, and the CycA concentration was kept fixed at 125 nM. Dose response curves are plotted at right. Average values for the maximum response (normalized to the maximum response in the absence of compound) or the k_d at each concentration across three replicates are plotted, and the error bars correspond to the standard deviation.

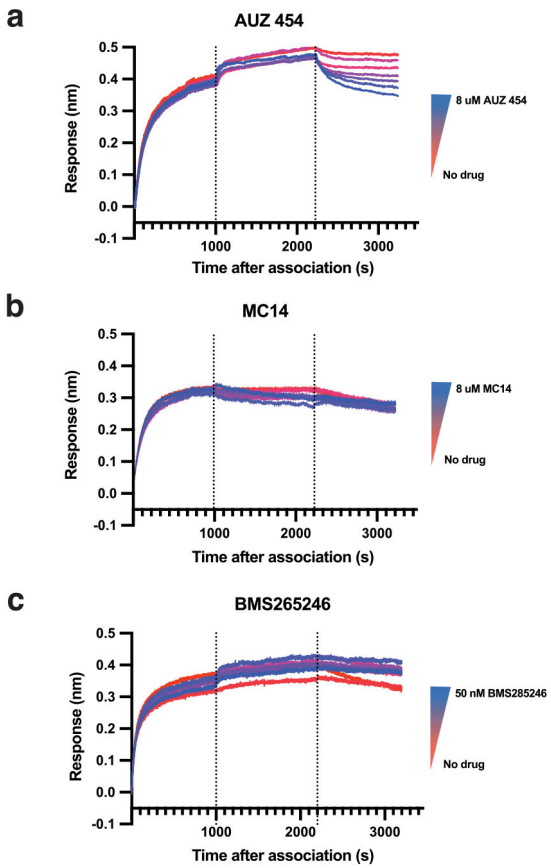

Figure 4.

Effects of the Cdk2 inhibitor when CycA added first to Cdk2. Dose response of (a) AUZ 454, (b) MC14, and (c) BMS265246 when Cdk2 is exposed to compound (middle step) only after CycA association (left step). CycA is kept in the middle step with the compound and then removed for dissociation (right step).

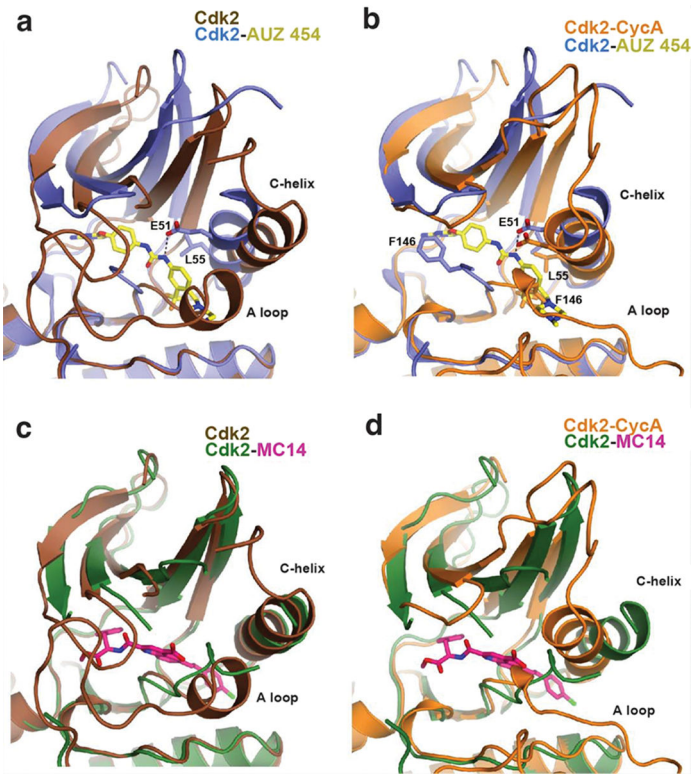

Figure 5.

Cyclin competitive compounds impose distinct structural perturbations to influence CycA binding kinetics. Structure of Cdk2-AUZ 454 (PDB: 5A14) aligned with (a) apoCdk2 (PDB: 1HCK) and (b) Cdk2-CycA (PDB: 1FIN). Structure of Cdk2-MC14 determined here aligned with (c) apoCdk2 and (d) Cdk2-CycA.